# Supplementary Material for: Modeling evidence for large, ENSO-driven interannual wintertime AMOC variability

**K. L. Smith**[1,3], **L. M. Polvani**[2,3]

[1] Department of Physical and Environmental Sciences, University of Toronto Scarborough, Toronto, Ontario, Canada
[2] Department of Applied Physics and Mathematics, Department of Earth and Environmental Sciences, Columbia University, New York, NY, USA
[3] Division of Ocean and Climate Physics, Lamont-Doherty Earth Observatory, Palisades, NY, USA

E-mail: karen.smith@utoronto.ca

## Contents



## Introduction

The following supplementary material includes text and figures outlining analysis for the WACCM4 integration. This analysis is complementary to that done for the CAM5 integration, discussed in the main body of the text.

## Text S1.

The leading EOF of the wintertime, January-February-March (JFM), AMOC in WACCM4 explains approximately 54% of the JFM AMOC variance, while the second and third EOFs explain 15% and 10%, respectively.

The correlation between the leading PC time series of the winter AMOC and the winter ENSO index in WACCM4 is also quite high and statistically significant at the 95% level ($R^2$=37.1%), while the correlation between the leading PC time series of the annual mean AMOC and the winter ENSO index is very low and not statistically significant ($R^2$=0.2%).

Finally, we find that the correlation between the leading PC time series of the winter AMOC and the winter NAO index in WACCM4 is statistically significant and similar to the correlation with the ENSO index ($R^2$=43.5%). Since the NAO is not independent of ENSO, this difference between WACCM4 and CAM5 may be due in part to the fact that the correlations between the ENSO and NAO indices differ between the two model integrations (correlation coefficients of -0.55 for WACCM4 and -0.35 for CESM).

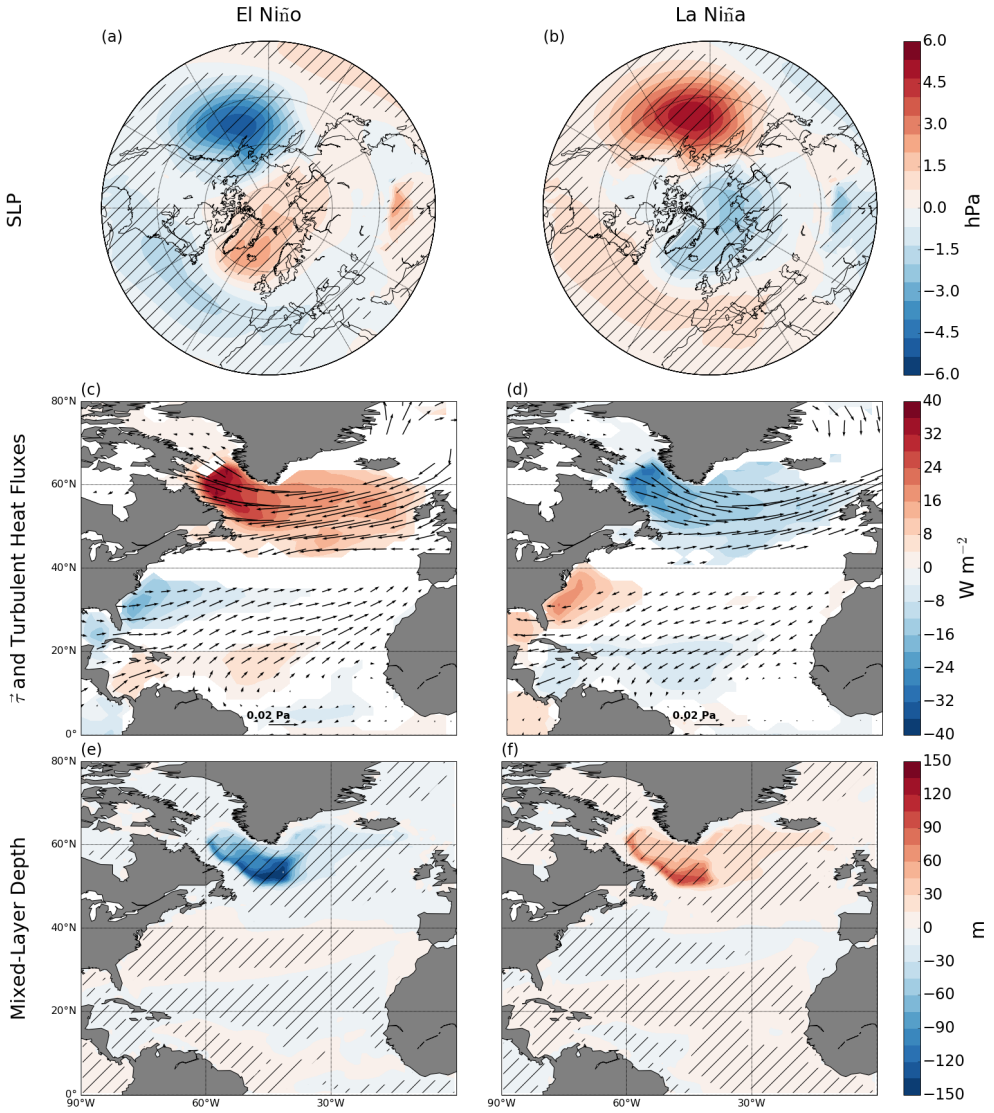


**Figure S1.** As in Figure 1, but for WACCM4. January-February-March (JFM) composites of El Niño (N = 117) and La Niña (N = 128) events in WACCM4. Top row: Polar stereographic sea level pressure (SLP) anomaly composites for El Niño (left column) and La Niña (right column) events. Middle row: North Atlantic surface wind stress ($\vec{\tau}$; vectors) and turbulent heat flux anomaly composites. Bottom row: North Atlantic mixed-layer depth anomaly composites. Statistical significance at the 95% level in the top and bottom rows is indicated by the hatching. In the middle row, only grid points that are statistically significant at the 95% level are either shaded or display a vector. Heat fluxes are positive into the ocean.

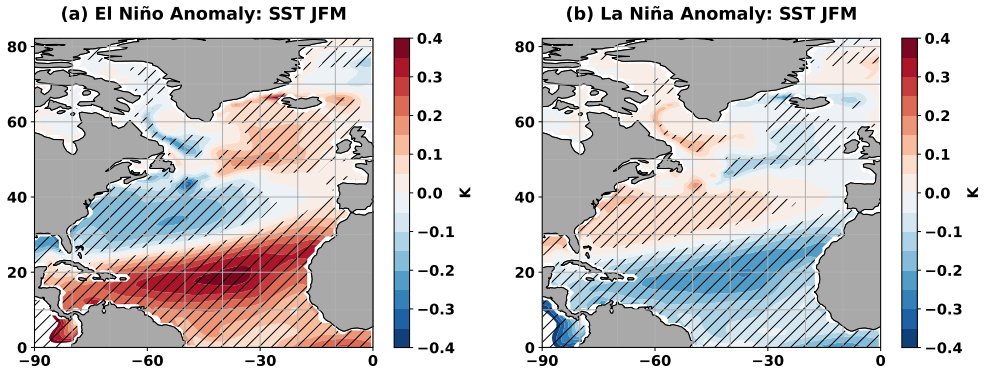


**Figure S2.** January-February-March (JFM) composites of North Atlantic sea surface temperature (SST) anomaly for El Niño (N = 281) and La Niña (N = 353) events in CAM5. Statistical significance at the 95% level is indicated by the hatching.

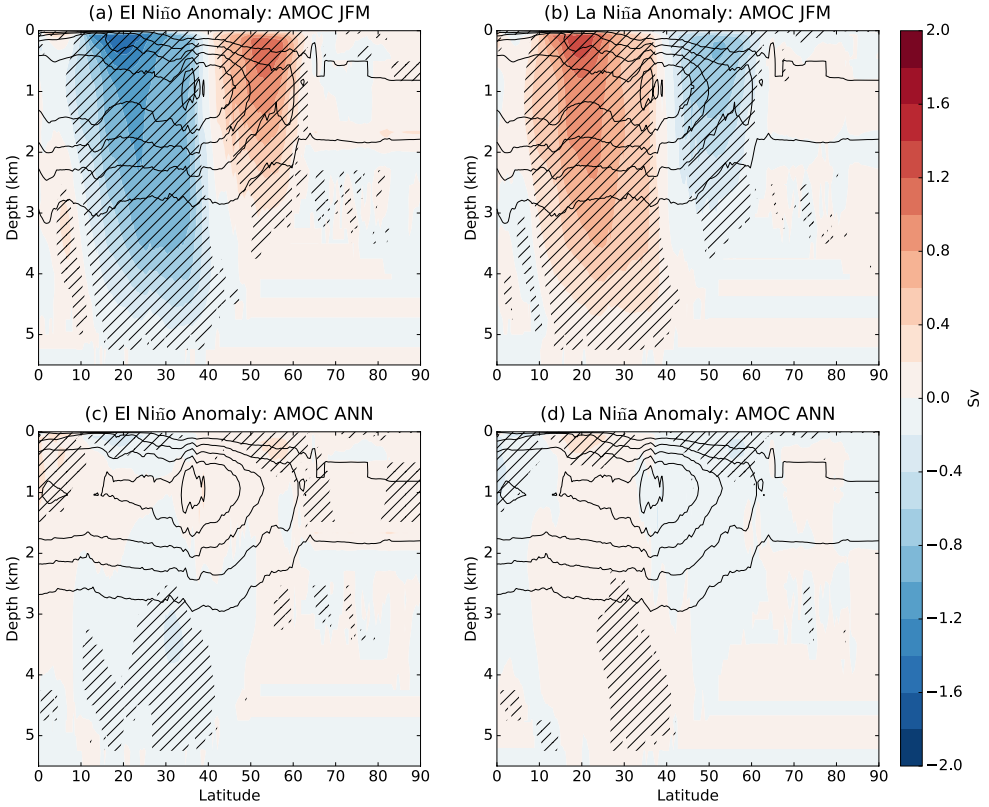


**Figure S3.** As in Figure 2, but for WACCM4. Top row: January-February-March (JFM) AMOC composites for (a) El Niño (N = 117; left column) and (b) La Niña (N = 128; right column) events in WACCM4 as a function of latitude and depth. The black contour indicates the climatological JFM AMOC streamfunction (contours are 5 Sv). Bottom row: Same as top row except for the annual mean AMOC. Statistical significance at the 95% level is indicated by the hatching.

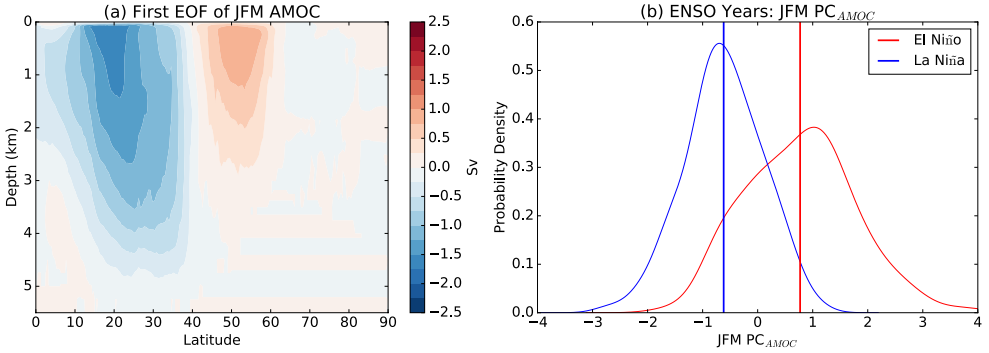


**Figure S4.** As in Figure 3, but for WACCM4. (a) Leading empirical orthogonal function (EOF) of the January-February-March (JFM) AMOC in WACCM4 as a function of latitude and depth. (b) Probability density distributions of the corresponding leading principal component (PC) time series of the January-February-March (JFM) AMOC for winters with El Niño (red; N = 117) and La Niña (blue, N = 128) events. The PC time series has been normalized, such that the units are in units of standard deviation. The vertical blue and red lines correspond to the composite mean PC values over the El Niño and La Niña events, respectively.